RESEARCH ARTICLE

Direct profiling and identification of peptide expression differences in the pancreas of control and ob/ob mice by imaging mass spectrometry

Laurens Minerva[1], Stefan Clerens[2], Geert Baggerman[3] and Lutgarde Arckens[1, 3]

[1] Laboratory of Neuroplasticity and Neuroproteomics, K.U.Leuven, Leuven, Belgium
[2] Protein & Structure, AgResearch Ltd, Christchurch, New Zealand
[3] Prometa, Interfaculty Center for Proteomics and Metabolomics, K.U.Leuven, Leuven, Belgium

Imaging mass spectrometry (IMS) technology utilizes MALDI MS to map molecules of interest in thin tissue sections. In this study, we have evaluated the potential of MALDI IMS to study peptide expression patterns in the mouse pancreas under normal and pathological conditions, and to *in situ* identify peptides of interest using MS/MS. Different regions of the pancreas of both control and ob/ob mice were imaged, resulting in peptide-specific profiles. The distribution of ions of *m/z* 3120 and 3439 displayed a striking resemblance with Langerhans islet's histology and, following MS/MS fragmentation and database searching were identified as C-peptide of insulin and glicentin-related polypeptide, respectively. In addition, a significant increase of the 3120 peak intensity in the obese mice was observed. This study underscores the potential of MALDI IMS to study the contribution of peptides to pancreas pathology.

Received: March 14, 2008
Revised: May 23, 2008
Accepted: May 26, 2008

Keywords:
Identification / *In situ* / MALDI IMS / Mouse / Pancreas

1 Introduction

In the past decade, proteomics has become an indispensable tool in biomedical research, traditionally combining high-resolution separation techniques and highly sensitive detection methods. Due to its high sensitivity and specificity, MS became the method of choice for the identification of relevant proteins and peptides in the context of a broad set of biological experiments [1]. Techniques such as MALDI MS [2, 3] combined with significant improvements to TOF mass spectrometers [4, 5] and advances in bioinformatics tools have revolutionized the ability to analyze the molecular composition of a given tissue specimen. The combination of MALDI MS with a separation technology such as 2-DE or LC are now routinely used to investigate complex protein mixtures following extraction [6–8]. Inevitably, the information regarding the spatial localization of the molecular components in the tissue is lost in this approach.

Imaging mass spectrometry (IMS) is a new technology that utilizes various MS techniques for the simultaneous mapping of many molecules present in thin tissue sections [9]. Specific information on the relative abundance and spatial distribution of each of the molecules is maintained, providing the opportunity to correlate ion-specific images with histological features observed by light microscopy. IMS represents an excellent discovery tool in research since the molecules recorded do not need to be known in advance and no label or reporter system is required to generate specific images [10, 11].

Protein profiling by IMS has been performed on human brain tumors [12–14], rat pituitary [15], mouse brain [16, 17], mouse prostate [18, 19], mouse epididymis [10],

Correspondence: Professor Lutgarde Arckens, Laboratory of Neuroplasticity and Neuroproteomics, K.U.Leuven, Naamsestraat 59, B-3000 Leuven, Belgium
E-mail: lut.arckens@bio.kuleuven.be
Fax: +32-16-324598

Abbreviations: DHB, 2,5-dihydroxybenzoic acid; **IMS,** imaging mass spectrometry; **IS,** ion source; **ROI,** region of interest; **SA,** 3,5-dimethoxy-4hydroxy-cinnamic acid or sinapinic acid

and in animal models for neurological disorders, including Parkinson's [20] and Alzheimer's disease [21]. In addition to the analysis of proteins, peptide profiling by IMS is also of biomedical relevance since peptides have been implicated in a variety of disease states. The different physiological functions of peptides, including feeding/body weight regulation, energy balance, memory and many others, underscore the importance of peptide imaging, as already performed on invertebrate neurons [22–26] and whole-body sections [27].

In this study, we therefore assessed different methodological refinements of a previously reported protein IMS method [17] to allow peptide detection in the m/z 1000–7000 range. Pancreas was the tissue of interest because of the large body of data on the presence of different peptides inside and outside the typical islets of Langerhans, as well as the implications of aberrant peptide distribution in different pancreatic diseases.

2 Materials and methods

2.1 Animals and tissue preparation

All experiments were conducted according to the European Communities Council Directive of 24 November 1986 (86/609/EEC), and carried out in accordance with institutional animal welfare guidelines (K.U.Leuven, Leuven, Belgium). These rules were followed strictly in all experiments. All efforts were made to minimize the animals' discomfort and to reduce the number of animals.

All experiments have been performed on pancreas of adult mice from the inbred C57Bl/6J strain obtained from Janvier Elevage (Le Genest-St-Isle, France; $n = 16$) and of homozygous ob/ob mice with a C57Bl/6J background ($n = 2$, kindly provided by A. Van den Berg; K.U. Leuven).

Animals were killed by cervical dislocation, the pancreas was rapidly removed and immediately frozen in liquid nitrogen cooled isopentane and stored at −80°C until sectioning in order to minimize peptide degradation caused by temperature and oxidation [28].

2.2 MALDI IMS

See workflow in Fig. 1 (for details on software see [29]).

2.2.1 Profiling

Ten micrometer-thick cryostat sections (Microm HM 500 OM, Walldorf, Germany) collected on the MALDI target plate (Bruker Daltonics, Bremen, Germany) were lyophilized for a minimum of 1 h. Two times 0.5 μL of matrix solution, with a 30 s interval, were pipetted on the tissue section. Matrix solutions were saturated solutions of three different matrices: CHCA, 3,5-dimethoxy-4hydroxy-cinnamic acid (SA), and 2,5-dihydroxybenzoic acid (DHB), dissolved in ACN/water/TFA, ethanol/water/TFA, or methanol/water/TFA in different concentrations ranging from 30 to 70% organic, with 0–2% TFA. Spectra were acquired in reflectron, positive mode with delayed extraction (50 ns) on an Ultraflex II MALDI-TOF/TOF mass spectrometer (Bruker Daltonics). Laser intensity was set around 70%, depending on the type of matrix, and the detector voltage at 1891 V. Each spectrum is the result of 150 consecutive shots at 66.7 Hz.

Experiments were performed with the ion source 1 (IS1) set to 25 kV, IS2 set to 21.6 kV, lens at 9.6 kV and Reflectrons 1 and 2 set at, respectively, 26.3 and 13.8 kV. No processing was performed on spectra from profiling analysis.

2.2.2 Imaging

Ten micrometer-thick cryostat sections collected on the MALDI target plate were lyophilized for a minimum of 1 h. The sections were spray-coated with matrix using a simple nebulizer (described in ref. [29]). The matrix solution was 50 mg/mL DHB (Acros Organics, Geel, Belgium) in 50% MeOH (HPLC grade, Riedel-deHaën, Hannover, Germany) in HPLC-grade water (Riedel-deHaën) with 0.1% TFA (99%, Acros Organics). Prior to spray coating, the tissue sections were covered with fine DHB seed crystals [29, 30].

An in-house developed program, *CreateTarget*, was used to create a geometry file describing a raster of sample points (at 100 μm resolution) according to the dimensions of the tissue section. This file was imported in the *FlexControl* software that controls the Bruker Ultraflex II mass spectrometer. This allowed the automated acquisition of spectra according to the defined grid. Spectra were calibrated using a mixture of Peptide Calibration Standard and Protein Calibration Standard I (m/z 1046, 1296, 1347, 1619, 2093, 2465, 3147, and 5734; Bruker Daltonics). An off-tissue calibration was used since no significant deviation between the detected masses of on- and off-tissue calibration was detected. With the same instrumental parameters as mentioned above in the profiling section spectra were acquired.

For image processing the *BioMap* software was used (http://www.maldi-msi.org). To allow import of the array of unprocessed raw spectra in *BioMap*, the spectra were converted to the Analyze 7.5 format using the *Analyze This!* software.

Overlay images were made in Photoshop CS2 (Adobe) by importing the IMS image (exported as a TIFF file from Analyze 7.5 format) and an analog photograph of the histology-stained tissue section taken *via* a Zeiss Axiophot 2 microscope under brightfield conditions (Zeiss MicroImaging, Oberkochen, Germany). Ion images with quantitative information are always accompanied by an unaltered color scale which was exported from Biomap (Figs. 2 and 3). Panels E and G of Fig. 2 and panels D and F of Fig. 3 lack a color scale in order to highlight the correlation between the ion images and their respective histology, and do not offer any information on relative intensities.

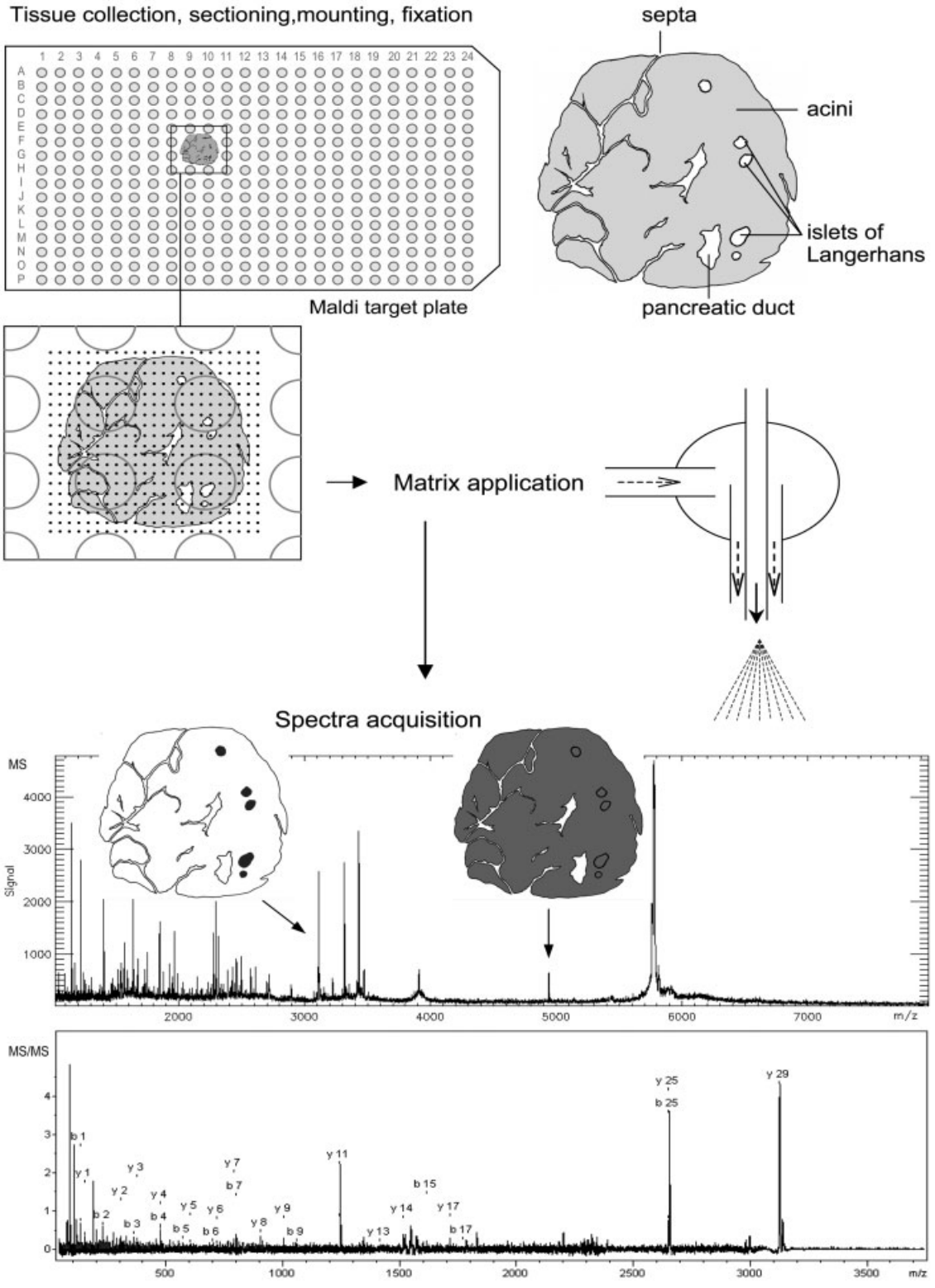

Figure 1. IMS workflow. Our MALDI IMS workflow indicating the necessary steps between tissue collection and imaging the distribution of an ion with a specific *m/z* value in a tissue section: tissue collection, sectioning and mounting of sections on the MALDI target plate, fixation, creating a raster using *CreateTarget* freeware, matrix application using a homebuilt nebulizer, spectrum acquisition on an Ultraflex II instrument using *FlexControl*, spectrum conversion into an image using *Analyze This!* and *BioMap*. Important landmarks for interpretation of pancreas data are indicated in the upper right drawing of a pancreas section.

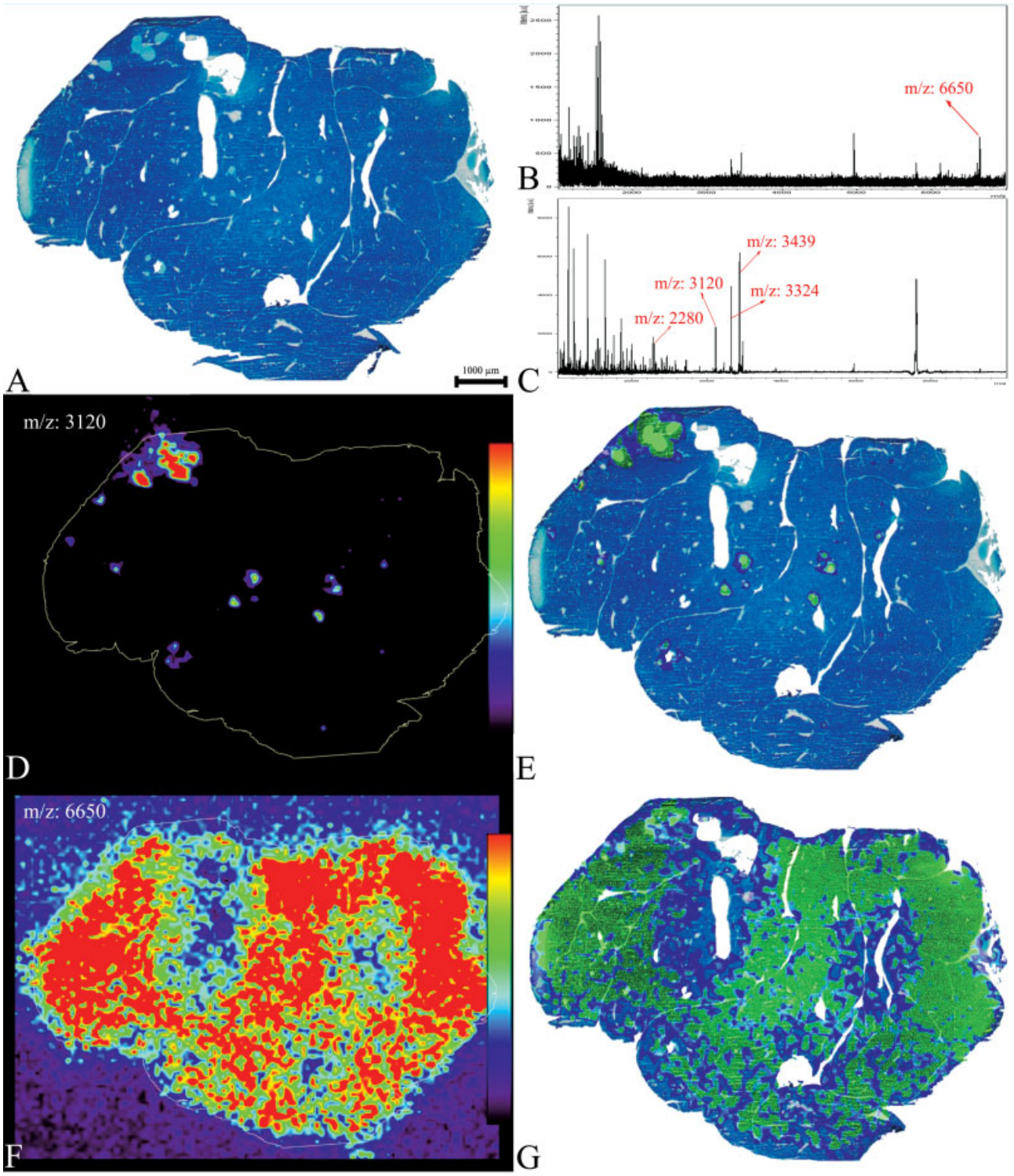

Figure 2. Peptide IMS of pancreatic tissue of normal mouse. (A) Methylene blue stained cryostat section of the pancreas. (B) Acini-specific spectrum. (C) Islet-specific spectrum. (D) IMS image for ion *m/z* 3120. (E) Overlay image of ion *m/z* 3120 and histology from panel A. (F) IMS image of ion *m/z* 6650. (G) Overlay image of *m/z* 6650 with histology. Note the good match between the islets, as detected based on the presence of *m/z* 3120, and the islets of Langerhans as detected with histology. Panels F and G present overlay images that clearly show that the ion image of *m/z* 6650 correlates with the acini, which comprises the bulk of the pancreas emphasizing the match between histology and the ion images. The color scale in panels D and F represent intensities with red as the highest and purple-black as the lowest. Ions with *m/z* 2280 and 3120 are relative lower expressed to *m/z* 3324 and 3439.

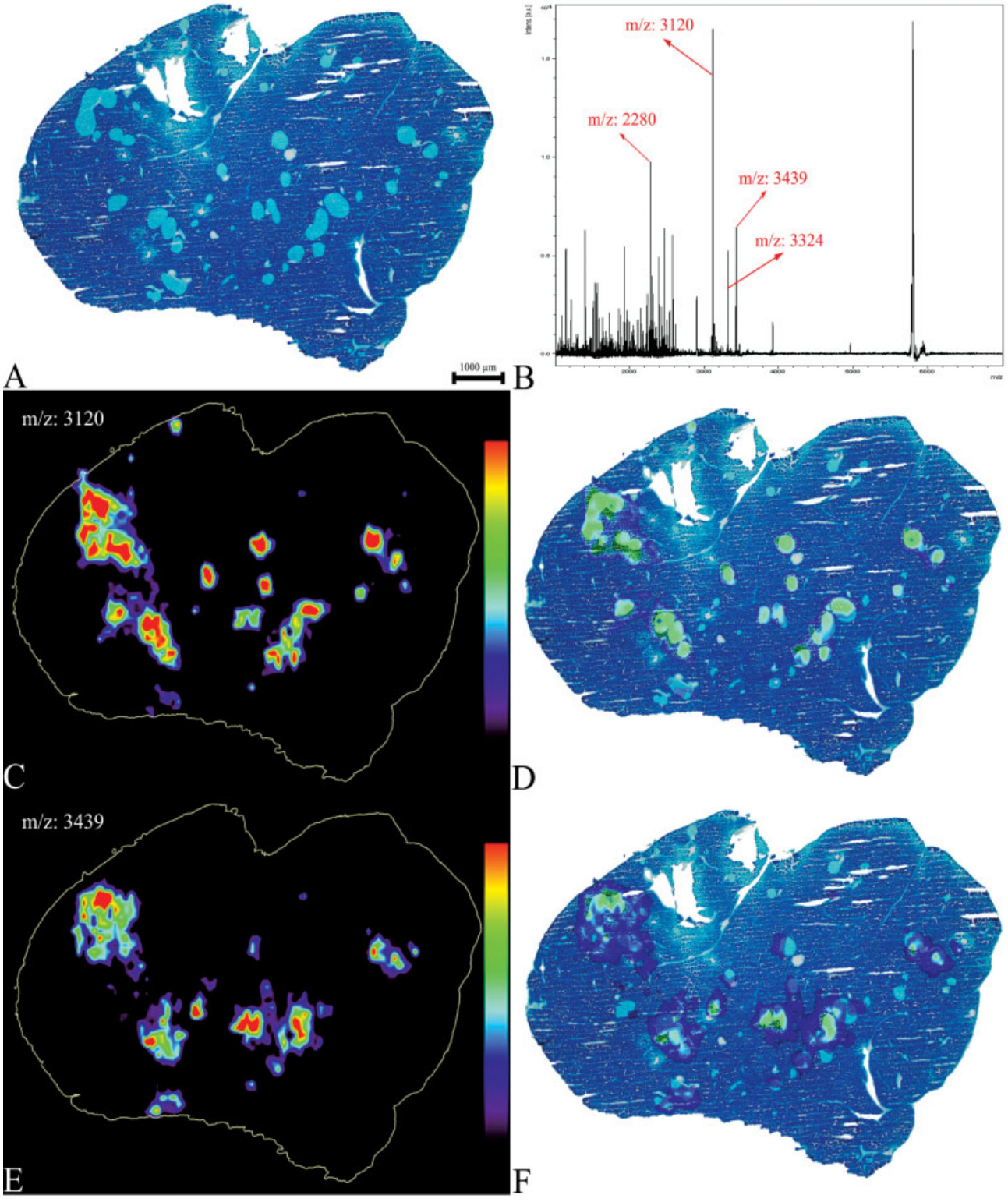

Figure 3. Peptide IMS of the pancreas of ob/ob mouse. (A) Methylene blue stained cryostat section of the pancreas. (B) Islet-specific spectrum. (C) IMS image for ion *m/z* 3120. (D) Overlay image of ion *m/z* 3120 and histology from panel A. (E) IMS image of ion *m/z* 3439. (F) Overlay image of *m/z* 3439 with histology. Note how more and larger islets appear for both ions, again nicely matching the islets as detected with histology. Ions with *m/z* 2280 and 3120 *versus m/z* 3324 and 3439 have a relative higher expression. Color scales are as in Fig. 2.

2.2.3 Identification

MS/MS spectra were acquired using the LIFT module on the Bruker Ultraflex II. All experiments were performed with the IS1 set to 8.00 kV, IS2 set to 7.15 kV, and LIFT 1 set to 19.00 kV and without DE. No collision gas was used. Settings for laser intensity were adjusted manually for optimal fragmentation.

A timed ion gate was used for precursor ion selection and the fragments generated were further accelerated in the LIFT cell, and detected following passage through the reflectron. For each fragmentation spectrum a total of 1000–1500 shots were acquired in 200-shot increments at a laser frequency of 200 Hz.

Processing of spectra in Biotools comprised baseline-subtraction (median) and smoothing (Savitzky-Golay filter). Peaks were detected by a SNAP algorithm and a peaklist was generated of the centroided (S/N 3) spectra.

Lift spectra were submitted to a database (Signpep, taxonomy: *Mus musculus,* http://peptides.statik.be; Feng, L., Baggerman, G., Schoofs, L., Wets, G., Construction of a database of signaling peptides in Metazoa. *In revision*) search on an in house MASCOT server (MASCOT 2.2, Matrix Science, London, UK). Enzyme specificity was set to *none* in order to identify native peptides. Variable modifications allowed for the presence of a C-terminal amide and methionine oxidation. Probability scores of 95% were used as a threshold for identification. All searches were performed with parent and fragment tolerance respectively set to 0.1 and 1 Da.

2.3 Histology

Methylene blue staining of adjacent pancreas sections was carried out according to standard procedures (1% solution in distilled water, 30 s) and was used to identify the size and position of different anatomical landmarks in the pancreas sections, including the islets of Langerhans.

3 Results

A first set of experiments was conducted to optimize the conditions for acquiring spectra of peptides in the 1–7 kDa range. For this purpose, tissue profiling was carried out using spotted matrix solution on mouse pancreas tissue sections. Saturated solutions of three different matrices (CHCA, SA, and DHB) dissolved in ACN/water/TFA, ethanol/water/TFA, or methanol/water/TFA in different concentrations ranging from 30 to 70% organic, with 0–2% TFA were evaluated (Table 1). No noticeable difference was observed for different TFA concentrations (0, 0.1, 0.5, 1, 2%). Conditions for which high quality spectra were observed included SA in 50–60% ACN, CHCA in 50–60% MeOH, DHB in 50–60% ACN, DHB in 30–50% MeOH, and DHB in 30% EtOH (Table 1).

Table 1. Summary table of profiling experiments

[%]	SA			CHCA			DHB		
	ACN	MeOH	EtOH	ACN	MeOH	EtOH	ACN	MeOH	EtOH
30	*X*	*X*	*X*	*X*	*X*	*X*	*X*	*V*	*V*
40	±	*X*	*X*	*X*	±	*X*	±	*V*	±
50	*V*	±	*X*	*X*	*V*	*X*	*V*	*V*	±
60	*V*	*X*	*X*	*X*	*V*	*X*	*V*	±	*X*
70	*X*	*X*	*X*	*X*	±	*X*	±	*X*	*X*

X represents conditions that resulted in spectra with little to no signals or a low signal intensity (low quality). Conditions creating high quality spectra are marked with a *V.* In some cases, only a few signals were detected or the intensity was diminished (low S/N). These spectra are represented by a ± and are of intermediate quality. The numbers in the left hand column signify the concentrations of the organic solvents which were used to prepare the various matrix solutions.

These conditions were further assessed in full IMS experiments. There, the best imaging results were generated with DHB in 50–60% ACN or 50–60% MeOH. The S/N for DHB in 50% ACN was marginally higher than with DHB in 50% MeOH. However, visual inspection of the matrix deposition quality showed that DHB in 50% MeOH produced a more homogeneous matrix layer, which had an advantageous effect on the reproducibility between sections.

In order to evaluate the effect of rinsing or rinsing/fixation, an acidic aqueous solution (H_2O/TFA, 99.9:0.1) and different EtOH solutions (75 and 90%) were applied prior to matrix application, and the IMS result compared with that of control tissue. The sample plate was held at an angle of 45° to rinse the tissue with 200 μL of washing/fixation solution. The control tissue displayed more peptide signals than either test condition, hence a rinsing or rinsing/fixation protocol was omitted from subsequent imaging experiments.

The effectiveness of the optimized peptide imaging method was further confirmed using a comparison of IMS and histologically stained sections of mouse pancreas. In the IMS-generated images of the pancreas of normal C57Bl/J mice, different ion peaks were found that showed a typical distribution pattern consistent with the islets of Langerhans *versus* the acini. Approximately 15 signals are acini-specific signals, 112 were only found in the islets of Langerhans and merely nine ion peaks are possible matrix related artifacts. Note that the islet- and acini-specific spectra, depicted in Figs. 2 and 3, are singe pixel based but represent the overall ion content of the islets and acini nonetheless. As illustrated in Fig. 2, ion m/z 3120 indeed displayed a density map that specifically resembled the islets throughout the pancreas. Other ions, for example m/z 6650, were clearly distributed throughout the acini (Fig. 2). Overlays of the IMS-generated images with photographs of methylene blue-stained adjacent sections clearly showed the high degree of overlap between anatomical features and marker ions, emphasizing that

minimal lateral dispersion, and representative and homogeneous extraction of analytes were achieved. In view of the great interest in the molecular mechanisms of pancreas disorders like pancreas cancer, diabetes, and obesity we then initiated an in depth study of these ions to determine the applicability of peptide IMS to generate new and relevant data with respect to our molecular understanding of these types of pathologies.

Imaging of pancreatic tissue from ob/ob mice was carried out according to the optimized protocol. Again adjacent tissue sections were methylene blue stained to provide histological landmarks for the interpretation of the resulting IMS images. Overall, the spectra for ob/ob pancreas showed good similarity to those of normal pancreas with most ion peaks lying in the m/z 1000–3000 range. By comparing spectra of the obese and normal condition, certain ion peaks appeared as differentially expressed. In obese pancreas, m/z 3120 was clearly higher expressed relative to m/z 3324 and 3439 (Fig. 3), opposite to our observations for normal pancreatic tissue (Fig. 2), and this was observed in four independent experiments. In the IMS-generated images for these ions, the number of islets detected was clearly higher than in the normal pancreas and the individual islets also appeared larger. This is in agreement with the histological data, which also revealed a higher number of islets of larger dimension (Fig. 3).

To allow direct identification of these ions of interest (m/z 3120, 3324, and 3439), an adjacent pancreatic tissue section was prepared for IMS. On this section, a region of interest (ROI) was determined, based on the coordinates of the histological landmarks and corresponding to an islet of Langerhans. In this ROI, MALDI-TOF/TOF MS/MS spectra were acquired directly from spray-coated tissue for ions m/z 3120, 3439, and 3324. The spectra were processed in Biotools and submitted for a MASCOT MS/MS ion search. m/z 3120 was identified as the C-peptide of insulin 1. m/z 3324 and 3439 were identified as the proglucagon cleavage product glicentin-related polypeptide, with m/z 3324 identical to m/z 3439 minus an aspartic acid at the N-terminus. Another ion with m/z 2280 in the ROI was identified as the C-peptide of insulin 2. Since they both are C-peptides, as expected m/z 2280 shares the same expression pattern as m/z 3120 *versus* m/z 3324 and 3439 (Figs. 2 and 3). The individual scores, expected values, observed and expected masses, and their sequences are presented in Table 2. Figures 4 and 5 depict the fragmentation spectra for each of the identified ions.

4 Discussion

The purpose of this study was to optimize an IMS protocol that facilitates investigating the distribution and identity of many peptides simultaneously in a given tissue, without the need for a reporter system or label, and without any prior knowledge on the peptides under study. Mouse pancreas was chosen as the subject of this study because of its abundance in peptides, in support of a swift method optimization as well as the availability of an extensive amount of literature about disease-related alterations in peptide expression.

4.1 Optimization of the peptide IMS method

Two kinds of experiments were set up. The effectiveness of different matrix solutions was first tested in a profiling experiment. Profiling allowed us to quickly evaluate different matrix compositions with regard to their efficacy in peptide extraction from tissue and peptide ionization on tissue. Solutions that generated (i) high peak resolution, and thus allowed to differentiate adjacent peaks; (ii) a set of ion signals representative of the molecular content of the tissue; and (iii) a high S/N, were then assessed more thoroughly in a set of imaging experiments. In these, the effects of rinsing and rinsing/fixation were also studied, and an additional criterion, the preservation of spatial distribution, was evaluated. Our research showed that in IMS experiments, peptides are subject to rapid delocalization. Rinsing and fixation steps prior to matrix application typically induced this problem and were therefore omitted from the protocol. Analysis of the eluates indeed revealed peptides in the rinsing and fixation solutions after tissue application. Also, matrix application is a compromise between maximizing the extraction of peptides and minimizing their delocalization. By optimizing the composition of the matrix solution and the nebulizer parameters, it was possible to achieve the application of a homogeneous matrix-coating on the total tissue section surface in a reproducible manner, with good peptide extraction and limited delocalization as witnessed by our overlay images for the C-peptide of insulin 1 and glicentin-related polypeptide, a processing product of proglucagon. Furthermore, the observation that many more peptides were detected in the islet-specific spectra as compared to acini-related spectra indicates that protein degradation is not an issue in our IMS spectra, as pancreatic acini are a rich source of high molecular weight proteins.

We succeeded in the identification of the four ions of interest by MS/MS analysis directly from tissue. This is a major breakthrough in IMS where up to now, identification of ions of interest has only been achieved using indirect methods, such as tissue extraction and peptide purification [32, 33], or *in situ* tryptic digestion followed by MS/MS [34, 35]. We have shown here that direct selection and analysis of an ion *via* MS/MS is feasible for molecules up to a mass of 3500 Da. To achieve this, optimization of the calibration of the IMS spectra was essential. The calibrant had to contain a protein of a molecular mass as close as possible to the ion subjected to identification.

Despite successful identifications obtained by *in situ* MS/MS analysis, many other ions were not identifiable due to their close spacing in the MS spectra which makes them difficult to select with the ion selector. FTICR-MS could address this issue and in combination with a broader array of

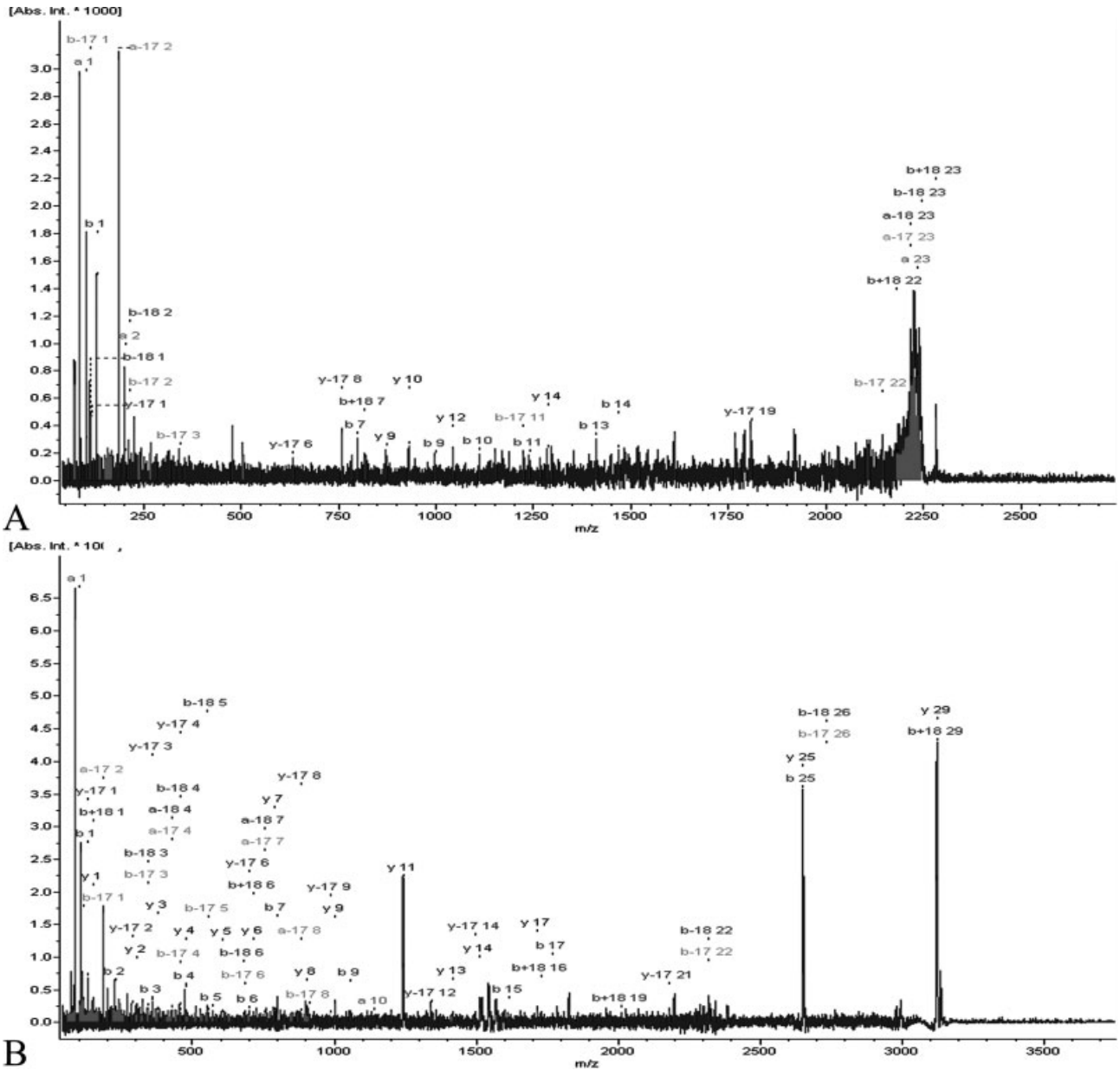

Figure 4. Fragmentation spectra. MS/MS spectra of ions with *m/z* (A) 2280 and (B) 3120. Ions are annotated according to standard nomenclature [31]. Annotation of internal fragments has been removed to reduce the complexity of the spectra.

identification techniques and unrivaled mass accuracy lead to more (accurate) identifications. Successful identifications by FTICR-MS directly on tissue have been reported [36, 37].

4.2 First application in a mouse model for diabetes and obesity

Disease mechanisms in obesity, diabetes, and pancreatic cancers remain poorly understood at the molecular level and no reliable peptidergic disease markers are available yet. Although animal models are extensively used to study etiology, pathogenesis, and new therapeutic approaches, only a limited number of proteomic studies have been published so far [38–41]. We initiated this MALDI IMS approach to perform an assessment of peptide patterns in different areas of the mouse pancreas to illustrate the potential of MALDI IMS to study mouse models of pancreas diseases to understand pathological disease mechanisms.

Ob/ob mice are hyperphagic, obese, hyperinsulemic and hyperglycemic and are used as a model for diabetes and obesity (for review, see [42]). The pancreas of ob/ob mice typically contains large islets of Langerhans with a volume

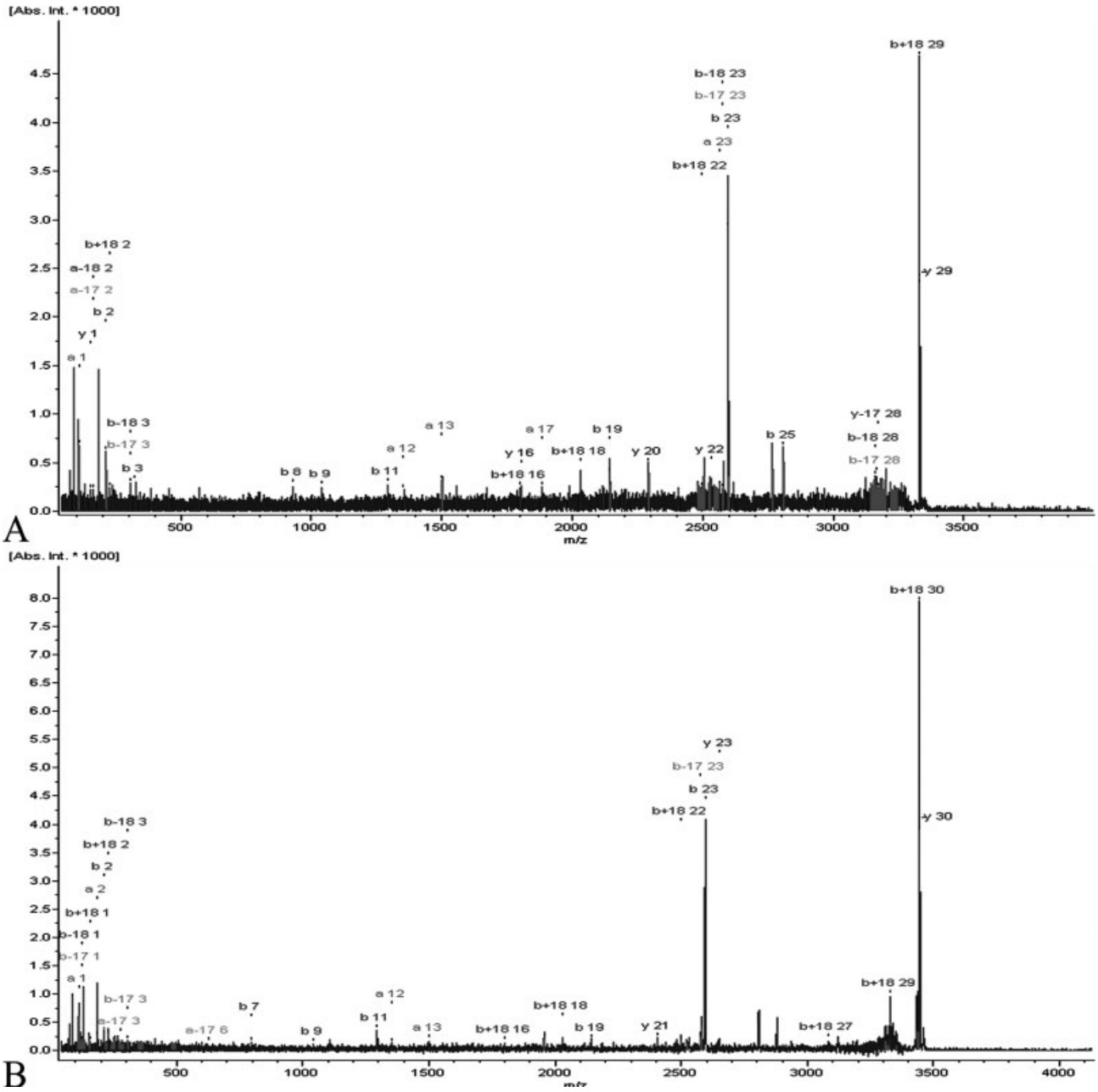

Figure 5. Fragmentation spectra. MS/MS spectra of ions with *m/z* (A) 3324 and (B) 3439. Annotation of fragments is as in Fig. 4.

up tot ten times higher than in normal mice. The hyperplasia is the consequence of an increased insulin demand and reflects a proportionally high number of insulin-producing beta-cells in the pancreatic islets. Our IMS observations perfectly fit these facts as more and larger islets were clearly imaged for the C-peptide ion.

By applying a peptidomics approach, Budde *et al.* [43] revealed increased levels of insulin, glucagon, amylin, proinsulin, C-peptide, and processing products of secretogranin, glucagon, and amylin when comparing the peptide content of islets extracts of obese *versus* lean mice. We here confirmed the altered expression of C-peptide, relative to glicentin-related polypeptide, using a combination of high resolution MALDI IMS and *in situ* identification using MS/MS fragmentation. Our spectra clearly show many more differences between the peptide content of normal and ob/ob mice that deserve attention in future research. In fact 52% of the peptides that are observed *via* a Q-TOF peptidomics approach in islet extracts [44] are also present in the islet-specific IMS spectra illustrating the degree of com-

Table 2. List of MS/MS identifications

m/z $[M + H]^+$	2280	3120	3324	3499
Score	26	35	41	28
Expectation values	0.011	0.0092	0.0048	0.0017
Observed mass	2280.51	3120.59	3324.49	3439.42
Expected mass	2279.51	3119.58	3323.48	3438.41
Id	c-Peptide of insulin 2	c-Peptide of insulin 1	Glicentin-related polypeptide	Glicentin-related polypeptide
Sequence	EVEDPQVAQLEL GGGPGAGDLQT	EVEDPQVEQLEL GGSPGDLQTLAL EVARQ	HALQDTEENPRS FPASQTEAHEDP DEMNE	HALQDTEENPRS FPASQTEAHEDP DEMNED

Note that the sequence of m/z 3324 is identical to m/z 3439 minus an N-terminal aspartic acid. m/z 2280 and 3120 are both C-peptides and expresses itself by sequence homology between the two ions.

plementarity between such different approaches. Indeed, a preliminary analysis reveals that the identification of peptides from Table 2 was identical to those of the related QTOF study [44].

Altogether our observations open new perspectives for applying MALDI IMS in future experiments concerning pancreas pathologies since we have illustrated that MALDI IMS is capable of detecting localized changes in peptide expression. In addition, MALDI IMS may be applied to study the delivery and distribution of therapeutic agents in pancreas tissue of different animal models for diverse pancreas disorders [33, 45–49].

5 Conclusion

MALDI IMS creates an excellent opportunity to correlate ion images and identities with anatomical and histochemical features and allows for the simultaneous mapping of several peptides in a certain tissue section within one experiment, without the need for highly specific antibodies or hybridization probes. We have clearly illustrated the power of MALDI IMS to study both normal and diseased pancreas. Correlating defects in the relative concentration and the subregional location of peptides to specific diseases such as obesity and diabetes will provide a more complete understanding of such disorders. Future IMS research may lead to the discovery of new disorder-specific peptide biomarkers with potential applications in disease diagnosis and classification.

We would like to acknowledge Lieve Geenen for expert technical assistance. This work was supported by the F.W.O. Flanders and the Research Council of the K.U. Leuven (0T 05/33). The authors would also like to thank the Flemish Government for the financing of the mass spectrometry facility ProMeta.

The authors have declared no conflict of interest.

6 References

[1] Rohner, T. C., Staab, D., Stoeckli, M., MALDI mass spectrometric imaging of biological tissue sections. *Mech. Ageing Dev.* 2005, *126*, 177–185.

[2] Hillenkamp, F., Karas, M., Beavis, R. C., Chait, B. T., Matrix-assisted laser desorption/ionization mass spectrometry of biopolymers. *Anal. Chem.* 1991, *63*, 1193A–1203A.

[3] Karas, M., Glückmann, M., Schäfer, J., Ionization in matrix-assisted laser desorption/ionization: Singly charged molecular ions are the lucky survivors. *J. Mass Spectrom.* 2000, *35*, 1–12.

[4] Brown, R. S., Lennon, J. J., Mass resolution improvement by incorporation of pulsed ion extraction in a matrix-assisted laser desorption/ionization linear time-of-flight mass spectrometer. *Anal. Chem.* 1995, *67*, 1998–2003.

[5] Vestal, M. L., Campbell, J. M., Tandem time-of-flight mass spectrometry. *Methods Enzymol.* 2005, *402*, 79–108.

[6] Roepstorff, P., Mass spectrometry in protein studies from genome to function. *Curr. Opin. Biotechnol.* 1997, *8*, 6–13.

[7] Aebersold, R., Goodlett, D. R., Mass spectrometry in proteomics. *Chem. Rev.* 2001, *101*, 269–295.

[8] Pandey, A., Mann, M., Proteomics to study genes and genomes. *Nature* 2000, *405*, 837–846.

[9] Chaurand, P., Schwartz, S. A., Reyze, M. L., Caprioli, R. M., Imaging mass spectrometry: Principles and potentials. *Toxicol. Pathol.* 2005, *33*, 92–101.

[10] Chaurand, P., Fouchécourt, S., DaGue, B. B., Xu, B. J. *et al.*, Profiling and imaging proteins in the mouse epididymis by imaging mass spectrometry. *Proteomics* 2003, *3*, 2221–2239.

[11] Caldwell, R. L., Caprioli, R. M., Tissue profiling by mass spectrometry: A review of methodology and applications. *Mol. Cell. Proteomics* 2005, *4*, 394–401.

[12] Stoeckli, M., Chaurand, P., Hallaha, D. E., Caprioli, R. M., Imaging mass spectrometry: A new technology for the analysis of protein expression in mammalian tissues. *Nat. Med.* 2001, *7*, 493–496.

[13] Schwartz, S. A., Weil, R. J., Johnson, M. D., Toms, S. A., Caprioli, R. M., Protein profiling in brain tumors using mass spectrometry: Feasibility of a new technique for the analysis of protein expression. *Clin. Cancer Res.* 2004, *10*, 981–987.

[14] Schwartz, S. A., Weil, R. J., Thompson, R. C, Shy, Y. *et al.*, Proteomic-based prognosis of brain tumor patients using direct-tissue matrix-assisted laser desorption ionization mass spectrometry. *Cancer Res.* 2005, *65*, 7674–7681.

[15] Caprioli, R. M., Farmer, T. B., Gile, J., Molecular imaging of biological samples: Localization of peptides and proteins using MALDI-TOF MS. *Anal. Chem.* 1997, *69*, 4751–4760.

[16] Crecelius, A. C., Cornett, D. S., Caprioli, R. M., Williams, B. *et al.*, Three-dimensional visualization of protein expression in mouse brain structures using imaging mass spectrometry. *J. Am. Soc. Mass. Spectrom.* 2005, *16*, 1093–1099.

[17] Ceuppens, R., Dumont, D., Van Brussel, L., Van de Plas, B. *et al.*, Direct profiling of myelinated and demyelinated regions in mouse brain by imaging mass spectrometry. *Int. J. Mass Spectrom.* 2007, *260*, 185–194.

[18] Todd, P. J., Schaaff, T. G., Chaurand, P., Caprioli, R. M., Organic ion imaging of biological tissue with secondary ion mass spectrometry and matrix-assisted laser desorption/ionization. *J. Mass Spectrom.* 2001, *36*, 355–369.

[19] Chaurand, P., Rahman, M. A., Hunt, T., Mobley, J. A. *et al.*, Monitoring mouse prostate development by profiling and imaging mass spectrometry. *Mol. Cell. Proteomics* 2008, *7*, 411–423.

[20] Pierson, J., Norris, J. L., Aerni, H. R., Svenningsson, P. *et al.*, Molecular profiling of experimental Parkinson's disease: Direct analysis of peptides and proteins on brain tissue sections by MALDI mass spectrometry. *J. Proteome Res.* 2004, *3*, 289–295.

[21] Stoeckli, M., Staab, D., Staufenbiel, M., Wiederhold, K. H., Signor, L., Molecular imaging of amyloid beta peptides in mouse brain sections using mass spectrometry. *Anal. Biochem.* 2002, *311*, 33–39.

[22] McDonnell, L. A., Piersma, S. R., Altelaar, A. F., Mize, T. H. *et al.*, Subcellular imaging mass spectrometry of brain tissue. *J. Mass Spectrom.* 2005, *40*, 160–168.

[23] Altelaar, A. F., van Minnen, J., Jiménez, C. R., Heeren, R. M. *et al.*, Direct molecular imaging of Lymnaea stagnalis nervous tissue at subcellular spatial resolution by mass spectrometry. *Anal. Chem.* 2005, *77*, 735–741.

[24] Rubakhin, S. S., Greenough, W. T., Sweedler, J. V., Spatial profiling with MALDI MS: Distribution of neuropeptides within single neurons. *Anal. Chem.* 2003, *75*, 5374–5380.

[25] Kruse, R., Sweedler, J. V., Spatial profiling invertebrate ganglia using MALDI MS. *J. Am. Soc. Mass Spectrom.* 2003, *14*, 752–759.

[26] DeKeyser, S. S., Kutz-Naber, K. K., Schmidt, J. J., Barrett-Wilt, G. A. *et al.*, Imaging mass spectrometry of neuropeptides in decapod crustacean neuronal tissues. *J. Proteome Res.* 2007, *6*, 1782–1791.

[27] Stoeckli, M., Staab, D., Schweitzer, A., Gardiner, J. *et al.*, Imaging of a beta-peptide distribution in whole-body mice sections by MALDI mass spectrometry. *J. Am. Soc. Mass Spectrom.* 2007, *18*, 1921–1924.

[28] Franzén, B., Yang, Y., Sunnemark, D., Wickman, M. *et al.*, Dihydropyrimidinase related protein-2 as a biomarker for temperature and time dependent post mortem changes in the mouse brain proteome. *Proteomics* 2003, *3*, 1920–1929.

[29] Clerens, S., Ceuppens, R., Arckens, L., CreateTarget and Analyze This!: New software assisting imaging mass spectrometry on Bruker Reflex IV and Ultraflex II instruments. *Rapid Commun. Mass Spectrom.* 2006, *20*, 3061–3066.

[30] Aerni, H. R., Cornett, D. S., Caprioli, R. M., Automated acoustic matrix deposition for MALDI sample preparation. *Anal. Chem.* 2006, *78*, 827–834.

[31] Roepstorff, P., Fohlman, J., Proposal for a common nomenclature for sequence ions in mass spectra of peptides. *Biomed. Mass Spectrom.* 1984, *11*, 601.

[32] Chaurand, P., Sanders, M. E., Jensen, R. A., Caprioli, R. M., Proteomics in diagnostic pathology: Profiling and imaging proteins directly in tissue sections. *Am. J. Pathol.* 2004, *165*, 1057–1068.

[33] Meistermann, H., Norris, J. L., Aerni, H. R., Cornett, D. S. *et al.*, Biomarker discovery by imaging mass spectrometry: Transthyretin is a biomarker for gentamicin-induced nephrotoxicity in rat. *Mol. Cell. Proteomics* 2006, *5*, 1876–1886.

[34] Groseclose, M. R., Andersson, M., Hardesty, W. M., Caprioli, R. M., Identification of proteins directly from tissue: *In situ* tryptic digestions coupled with imaging mass spectrometry. *J. Mass Spectrom.* 2007, *42*, 254–262.

[35] Shimma, S., Sugiura, Y., Hayasaka, T., Zaima, N. *et al.*, Mass imaging and identification of biomolecules with MALDI-QIT-TOF-bases system. *Anal. Chem.* 2008, *80*, 878–885.

[36] Kutz, K. K., Schmidt, J. J., Li, L., *In situ* analysis of neuropeptides by MALDI FTMS in-cell accumulation. *Anal. Chem.* 2004, *76*, 5630–5640.

[37] Taban, I. M., Altelaar, A. F., van der Burgt, Y. E., McDonnell, L. A. *et al.*, Imaging of peptides in the rat brain using MALDI-FTICR mass spectrometry. *J. Am. Soc. Mass Spectrom.* 2007, *18*, 145–151.

[38] D'Hertog, W., Overbergh, L., Lage, K., Ferreira, G. B., Maris, M. *et al.*, Proteomics analysis of cytokine-induced dysfunction and death in insulin-producing INS-1E cells: New insights into the pathways involved. *Mol. Cell. Proteomics* 2007, *6*, 2180–2199.

[39] Sanchez, J. C., Chiappe, D., Converset, V., Hoogland, C. *et al.*, The mouse SWISS-2D PAGE database: A tool for proteomics study of diabetes and obesity. *Proteomics* 2001, *1*, 136–163.

[40] Chen, R., Yi, E. C., Donohoe, S., Pan, S. *et al.*, Pancreatic cancer proteome: The proteins that underlie invasion, metastasis and immunologic escape. *Gastroenterology* 2005, *129*, 1187–1197.

[41] Chen, R., Pan, S., Cooke, K., Moyes, K. W. *et al.*, Comparison of pancreas juice proteins from cancer *versus* pancreatitis using quantitative proteomic analysis. *Pancreas* 2007, *34*, 70–79.

[42] Lindström, P., The physiology of obese-hperglycemic mice (ob/ob mice). *ScientificWorldJournal* 2007, *7*, 666–685.

[43] Budde, P., Schulte, I., Appel, A., Neit, S. *et al.*, Peptidomics biomarker discovery in mouse models of obesity and type 2 diabetes. *Comb. Chem. High Throughput Screen.* 2005, *8*, 775–781.

[44] Boonen, K., Baggerman, G., D'Hertog, W., Husson, S. J. *et al.*, Neuropeptides of the islets of Langerhans: A peptidomics study. *Gen. Comp. Endocrinol.* 2007, *152*, 231–241.

[45] Rubakhin, S. S., Jurchen, J. C., Monroe, E. B., Sweedler, J. V., Imaging mass spectrometry: Fundamentals and applica-

tions to drug discovery. *Drug Discov. Today* 2005, *10*, 823–837.

[46] Chaurand, P., Schwartz, S. A., Capriol, R. M., Assessing protein patterns in disease using imaging mass spectrometry. *J. Proteome Res.* 2004, *3*, 245–252.

[47] Hsieh, Y., Casale, R., Fukuda, E., Chen, J. *et al.*, Matrix-assisted laser desorption/ionization imaging mass spectrometry for direct measurement of clozapine in rat brain tissue. *Rapid Commun. Mass Spectrom.* 2006, *20*, 965–972.

[48] Reyzer, M. L., Hsieh, Y., Ng, K., Korfmacher, W. A., Caprioli, R. M., Direct analysis of drug candidates in tissue by matrix-assisted laser desorption/ionization mass spectrometry. *J. Mass Spectrom.* 2003, *38*, 1081–1092.

[49] Troendle, F. J., Reddick, C. D., Yost, R. A., Detection of pharmaceutical compounds in tissue by matrix-assisted laser desorption/ionization and laser desorption/chemical ionization tandem mass spectrometry with a quadrupole ion trap; *J. Am. Soc. Mass Spectrom.* 1999, *10*, 1315–1321.

